

Article

Scheduling and Path-Planning for Operator Oversight of Multiple Robots

Sebastián A. Zanlongo¹, Peter Dirksmeier², Philip Long³, Taskin Padir², Leonardo Bobadilla¹

¹ Knight Foundation School of Computing and Information Sciences, Florida International University; szanl001@fiu.edu, bobadilla@cs.fiu.edu

² Department of Electrical and Computer Engineering, Northeastern University; dirksmeier.p@husky.neu.edu, t.padir@northeastern.edu

³ Robotics & Automation Department, Irish Manufacturing Research; philip.long@imr.ie

* Correspondence: philip.long@imr.ie

Version July 31, 2021 submitted to *Robotics*

Abstract: There is a need for semi-autonomous systems capable of performing both automated tasks and supervised maneuvers. When dealing with multiple robots or robots with high complexity (such as humanoids), we face the issue of effectively coordinating operators across robots. We build on our previous work to present a methodology for designing trajectories and policies for robots such that few operators can supervise multiple robots. Specifically, we: 1) Analyze of the complexity of the problem, 2) Design a procedure for generating policies allowing operators to oversee many robots, 3) Present a method for designing policies and robot trajectories to allow operators to oversee multiple robots, and 4) Include both simulation and hardware experiments demonstrating our methodologies.

Keywords: Human Robot interaction; Multi-robot coordination; Humanoid Robots; Scheduling and Coordination ; Supervisory Control

1. Introduction

Multi-robot systems are making a significant impact on fundamental societal areas. From oceanic exploration to border surveillance, from robotic warehousing to precision agriculture, and from automated construction to environmental monitoring, collaborating groups of robots will play a central role in the coming years [1]. In some of these scenarios, however, due to technical, ethical, regulatory or safety issues [2], one or more humans should monitor or help the robot during the execution of its tasks in certain critical parts. These critical segments of the robot trajectory can be kinematically or dynamically complex maneuvers, locations near obstacles, or regions where sensing is poor.

Most teleoperated systems assume more than one human operator per robot. More than a human may be required for each subsystem in more complex scenarios, such as humanoids or mobile manipulator teleoperation (e.g., manipulation, locomotion, head positioning). For instance, in control rooms in Unmanned Aerial Vehicles missions, several operators are needed to operate a single drone. While it may remain infeasible to remove altogether the portion of a task which cannot be automated, we can efficiently allocate human *attention* in these portions. As an application of our ideas, we envision scenarios where a single operator can coordinate a group of automated construction machinery, several agricultural pieces of equipment or even a production line of industrial robots. Indeed, the recent pandemic has demonstrated teleoperation control paradigms are favoured in situations where remote presence is desirable and where complexity precludes the use of fully autonomous systems [3]. Effectively combining the cognitive capabilities of a human operator with

31 robot physical capacities [4] has provided great benefits in industrial applications [5,6] and more
32 general methodologies are needed.

33 Another motivation behind our ideas is *robot-assisted search and rescue*. In traditional mobile robot
34 search and rescue operations using unmanned vehicles, operators' ratio to robots is commonly 2 to
35 1 [7]. More recently, motivated by disasters such as the Fukushima nuclear plant, there has been a
36 need for robots with larger degrees of freedom that can operate in environments designed for humans.
37 Concretely, lessons learned analyzing human-robot interfaces used by different teams in the DARPA
38 Robotics Challenge (DRC) [8], gave two important reasons motivating our ideas to reduce the number
39 of operators: 1) fewer operators reduces confusion and coordination overhead, and 2) the amount of
40 human errors (one of the main sources of problems in the DRC [9]) is reduced.

41 **This work addresses the question of operator attention at critical moments of a teleoperation**
42 **task**. In most situations, an operator is only required in specific parts of a robot's operation. Knowing
43 this, we can schedule these operator interactions so that a single operator can perform multiple tasks.
44 **Thus, our objective is to develop a planning strategy for the remote task involving multiple robots**
45 **such that the operator can pay sufficient attention to each robot during critical operations**. This work's
46 contributions are: extending our preliminary ideas from [10,11] in the following directions: First, we
47 analyze the complexity of this problem. Secondly, we present a sampling-based approach that allows
48 us to design policies for many teleoperators instead of a complete algorithm that only works for a small
49 set of operators. Thirdly, we allow re-planning of the robot's task alongside the operator. Finally, we
50 present the results of both simulated and physical experiments using mobile robots and a humanoid.

51 Our work deals with planning for robots using a small set of operators that can help the robot
52 when needed. As a convention, we will use the term "robot" throughout this paper; however, the
53 method is formulated within the robots' configuration space and is agnostic to the robot type. It can
54 model multiple robots and a single robot with multiple degrees of freedom such as a humanoid robot.
55 To the best of our knowledge, our contribution is one of the few that attempts to formalize operator
56 scheduling problem using a geometric approach.

57 The rest of the paper is organized as follows: Section 2 discusses relevant related literature. Section
58 3 describes the preliminaries and formulates the problems of interest. Section 4 describes algorithms
59 to solve the formulated problems in the previous section. In Section 5, we present an extension of
60 the solution in Section 4 which can also re-plan robot trajectories. Section 6 presents both software
61 and hardware experimental results, and a case study is provided in Section 7. Conclusions and future
62 directions are presented in Section 8.

63 2. Related Work

64 Teleoperation is an established robot control paradigm with particular widespread use in surgical
65 and **medical operations** [12]. While teleoperation is classically defined using 1 : 1 operator to robot
66 ratio [13,14], there is a growing need for systems that facilitate operator oversight of multiple robots [15].
67 This work focuses on reducing operator supervision to only temporally critical passages. Previous
68 work has taken a different approach, aiming to reduce the cognitive burden on the operator by, for
69 instance, using virtual fixtures [16,17]. Virtual fixtures create zones where the robot can operate and
70 thus reduce the operators' supervision load. These zones can be obtained using point cloud data [18],
71 shape primitives, [19], manually created [20], **selected interactively** [21] or generated on-line based on
72 obstacle proximity and manipulator capabilities [22]. For the teleoperation of multiple agents, [23]
73 proposed a discrete switching control algorithm where an operator can trigger a switch to control
74 different robots or different inputs, i.e. position, velocity of the same agent. In [24], the authors propose
75 modeling operator behavior in a multi-robot control task and hypothesize that these models can be
76 used to improve the teleoperation control strategies. Alternatively, for more complex systems, the
77 introduction of a degree of autonomy in the robots' behavior, often denoted as shared control, can
78 enable operators to control multi-agent or complex systems [25]. Utilizing operators alongside partially
79 autonomous robots yields systems that are less brittle and more effective than either one working

80 alone [26]. A study case of a foraging task is presented in [27] where queuing techniques were used to
 81 schedule the operator's attention. In [28] the output side sensor configuration of a teleoperated system
 82 is altered to reduce the workload of a remote surgeon.

83 While the above techniques enhance the operators' control of a robot system, we focus on complex
 84 autonomous systems that *require* supervision and analyse how this supervising burden may be reduced.
 85 Using one operator to control multiple robots has benefits in terms of cost and control coherency but
 86 leads to a higher workload and decrease in situation awareness [29]. The human operator is often
 87 overlooked when supervising robots [30], despite their workload influencing task performance [31]
 88 and in fact having long-term negative effects on well-being [32]. Indeed, [33] have demonstrated that
 89 an increase in the number of robots per human significantly degrades performance and situation
 90 awareness. An increase in supervision burden has been shown to increase accidents during multi-robot
 91 control trials [34]. While this may be mitigated by smart alert systems [35,36], it has been shown
 92 in [37] that too many robot systems will eventually saturate operator capabilities and, in turn, lead
 93 the operators to neglect some robots. Neglect is mainly due to the robots competing for operator
 94 attention [38]. In [39], the authors propose real-time measurements of neurophysiological parameters
 95 to estimate workload as a potential input to new forms of adaptive automation.

96 Our work focuses on eliminating this failure mode by judicious scheduling events that are likely
 97 to require concentrated operator attention.

98 We build upon our recent work [10,11], to perform multi-robot planning [40,41]. We also find
 99 complementary goals in [42] where a robot attempts to move from one location in its environment to
 100 another by calculating which obstacles can be minimally displaced to generate a feasible trajectory.
 101 In our work, we will similarly generate a coordination space, where operator "collision obstacles"
 102 must be avoided, and seek to find the minimal displacement needed to avoid them. In work by
 103 LaValle and Hutchinson [43,44], as well as by Wang et al. [45], the complexity of coordinating both
 104 many robots and operators is handled by separating the planning and scheduling aspects into two
 105 separate steps. This division greatly assists in devising a feasible solution and is echoed here as
 106 well. Our work develops techniques for planning multi-robot missions that can assist in outlining
 107 mission requirements and robot policies. There are relevant approaches such as Crandall et al. [46]
 108 which investigates the effects of allocating operator attention to robots, and [47–49] which investigate
 109 additional methods of distributing operators across robots and the effects this has. Particularly relevant
 110 to our research ideas are [50,51] where the expected behaviors of humans in an environment are
 111 incorporated into the planning phase of robots, allowing them to perform more elaborate plans than
 112 without this prediction. This argument also extends into more industrial settings, where it is often
 113 repeated, scheduled interaction between robots and operators [5]. Our work also relates to motion
 114 planning approaches that generate joint plans for humans and robots [52–54].

115 3. Preliminaries

116 We start with a set of m of bodies, which can be kinematic chains or mobile robots, $\mathcal{A} =$
 117 $\{\mathcal{A}^1, \dots, \mathcal{A}^m\}$. Each robot $\mathcal{A}^i \in \mathcal{A}$ has a configuration space \mathcal{C}^i representing the set of all possible
 118 transformations, where the set of valid configurations is called the free space \mathcal{C}_{free}^i . Robots also have
 119 initial $q_I^i \in \mathcal{C}_{free}^i$ and goal $q_G^i \in \mathcal{C}_{free}^i$ configurations, where the trajectory $\lambda^i : [0, t_f^i] \rightarrow \mathcal{C}_{free}^i$ takes the
 120 robot from $\lambda^i(0)$ - corresponding to q_I^i - through \mathcal{C}_{free}^i to the final configuration $\lambda^i(t_f^i)$ - corresponding
 121 to q_G^i , where t_f^i is the total runtime for \mathcal{A}^i to execute λ^i given a dedicated operator.

122 When executing λ^i , \mathcal{A}^i may enter critical configurations $\mathcal{C}_{att}^i \subset \mathcal{C}_{free}^i$ during which it will require
 123 one of the p operator's supervision. A conflict occurs when more than p robots require supervision at
 124 the same time. Given a range of time $T = [0, t_f]$ where the mission is executing, we will attempt to
 125 minimize $t_f = \max(t_f^1, \dots, t_f^m)$ when all robots have finished, while also providing operator attention
 126 when required.

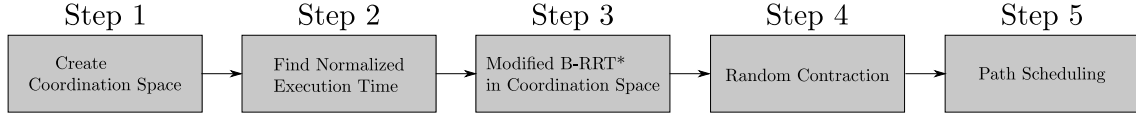


Figure 1. Overall steps involved in the proposed scheduling approach.

127 Problem 1: Scheduling for Multiple Operators: Given p the number of operators, a set of robots \mathcal{A} -
128 each with their trajectories λ^i , and a set of critical configurations \mathcal{C}_{att}^i - determine a policy $\pi^i : T \rightarrow \mathcal{C}_{free}^i$ for
129 each robot such that 1) all robots are only in critical configurations when an operator can supervise them, 2) the
130 number of operators requested at any time does not exceed p , and 3) attempt to reduce the total runtime of the
131 mission t_f .

132 Building on this problem, we can add the following condition: Is it possible to yield a shorter
133 mission runtime by generating alternative trajectories for bodies such that they do not require
134 supervision simultaneously as other robots in the first place, thus avoiding operator attention
135 "collisions" altogether? This question leads us to a concrete extension of Problem 1:

136 Instead of a pre-determined trajectory, we use a sequence of waypoints $\tau^i = [\tau_1^i, \dots, \tau_o^i]$ - where
137 each waypoint is a specific configuration the robot must achieve, and the application-specific function
138 $plan(A^i, \tau^i, t_{den})$ yields a trajectory that visits τ^i while avoiding \mathcal{C}_{att}^i during operator-denied times t_{den}
139 - an example of which can be found in Section 6.

140 Problem 2: Scheduling with Re-Planning: Given p operators, a set of robots \mathcal{A} each with a sequence
141 of sub-goals τ^i , and a set of critical configurations \mathcal{C}_{att}^i . Determine a trajectory λ^i and policy $\pi^i : T \rightarrow \mathcal{C}_{free}^i$ for
142 each robot satisfying the waypoints such that 1) robots are in critical configurations only when an operator can
143 supervise them, 2) the number of operators requested at any time is less than or equal to p , and 3) an effort is
144 made to minimize the ending time of the mission t_f .

145 4. Scheduling Operator Attention

146 This section will propose solutions to Problem 1 defined in Section 3. A schematic representation
147 of the steps of our approach is outlined in Figure 1. Details of the method will be explained below.

148 4.1. Computational Complexity of Scheduling for Multiple Operators

149 In our previous work [11], we described the operator scheduling problem and presented a
150 geometric approach for its solution. There were several issues with the proposed methodology related
151 to the computational complexity of creating the entire set of obstacles with the coordination space. To
152 solve this problem, we give a proof sketch proving the complexity of this problem.

153 We prove that Problem 1 is NP-Hard by using the technique of *restriction* ([55], pg 63). An
154 NP-Hardness proof by restriction consists of showing that a problem Π (in our case, Problem 1)
155 contains a known NP-Hard Π' as a special case.

156 In our proof, Π' is the *Multiprocessor Scheduling* problem ([55], pg 238), which consists of a set of
157 J jobs, each job j^i has a corresponding length l^i . Given p processors, we must schedule this set of jobs
158 so that they 1) do not overlap and 2) execute in the minimum amount of time.

159 Starting from problem 1 (our operator scheduling problem), assume that all possible
160 configurations for the robot will require operator attention, meaning that the entire execution of
161 λ^i will need an operator. This plan's runtime is t_f^i , and is analogous to the length of a job in the original
162 Multiprocessor Scheduling problem. These jobs are scheduled and allocated to p operators, which
163 would be the processors in the original formulation. This problem then reduces to the Multiprocessor
164 Scheduling problem where we schedule j jobs across p processors and indicates that the problem we
165 are trying to solve is NP-hard.

166 4.2. A sampling-based solution

167 Knowing that the problem is NP-hard we ask, we will propose heuristics to find feasible solutions.

168 We start by by creating a *Coordination Space* $X = [0, \tilde{t}_f^1] \times \dots \times [0, \tilde{t}_f^m]$ (following a procedure
169 similar to [56]) representing all possible configurations of the robots along their trajectories. Each of170 the m axes corresponds to the normalized execution time \tilde{t}_f^i of robot \mathcal{A}^i , given by $\tilde{t}_f^i = \frac{t_f^i}{\max(t_f^1, \dots, t_f^m)}$,171 with the position along the axis corresponding to progress along the trajectory. Let X_{obs} be the
172 set of invalid configurations where the number of robots requesting supervision exceeds p , and173 $X_{free} = X \setminus X_{obs}$ be the set of all valid configurations where the number of requests does not exceed p .174 At $x_{init} = (0, \dots, 0) \in X_{free}$ all robots are in their initial configurations, and at $x_{goal} = (\tilde{t}_f^1, \dots, \tilde{t}_f^m) \in X_{free}$
175 all robots are in their final configuration.176 We define auxiliary functions, borrowing the notation from [57]: $d(x_1, x_2)$ is the Euclidean distance
177 between two points, and $c(\cdot)$ is the cost of a path corresponding to the sum of the pairwise Euclidean
178 lengths of the pairwise linear points within it.179 The above formulation serves to create a coordination space where the position along axes
180 represents robot configurations and invalid configurations where multiple robots request obstacles
181 represent an operator. This process allows us to convert the coordination problem into a path-planning
182 problem. We must find a path $h : [0, 1] \rightarrow X_{free}$ from $h(0) = x_{init}$ to $h(1) = x_{goal}$. Following h will
183 give us an implicit representation of time with each robot's positions along their trajectory, such that
184 each robot will move from its initial state to its goal state, with at most p robots requiring operator
185 attention. We performed this calculation by mapping h to the trajectory λ^i corresponding to a particular
186 robot. Define $\sigma : h \rightarrow [0, \tilde{t}_f^i]$, which indicates the position of the robot along its trajectory λ^i at the
187 corresponding point of path h through X_{free} . We then perform the composition $\phi : \lambda \circ \sigma$, which yields
188 $\phi : h \rightarrow \mathcal{C}_{free}$, mapping from the path h to \mathcal{C}_{free} . This allows us to determine the configuration of a
189 robot at any point q in h via $\phi(q) = \lambda(\sigma(q))$. We can now obtain the series of configurations \tilde{x} for each
190 robot that will guarantee that at most p robots require operator attention at any given time and reduces
191 the total run-time of the mission.192 Our preliminary solution [11] required generating the entire set of obstacles within the
193 coordination space. Here, we instead use a lazy approach which only checks sampled locations.
194 This is combined with a modified version of the Bidirectional RRT^* originally described in [57–59],
195 and shown in Algorithm 2 for reference. Define graphs $\mathcal{G}_a = (V_a = \{x_{init}^a\}, E = \emptyset) \in X_{free}$,
196 $\mathcal{G}_b = (V_b = \{x_{init}^b\}, E = \emptyset) \in X_{free}$, where $x_{init}^a = x_{init}$ and $x_{init}^b = x_{goal}$. The objective will be to
197 derive an obstacle-free path $h : [0, 1] \rightarrow X_{free}$ such that $h(0) = x_{init}, h(1) = x_{goal}$. Given a user-defined
198 function that can estimate when robots will enter a critical section $\mathcal{S} \leftarrow \text{CriticalSegments}(A)$ we can
199 check if a point $x \in X$ is obstacle-free as in Algorithm 1, where for the point being evaluated, we iterate
200 over each robot's critical segments (lines 3, 4) and check if the corresponding axis of x lies within the
201 segment (line 5). If the number of collisions is greater than the number of operators (line 7), then the
202 location is not obstacle-free. With some abuse of notation, we also use this to refer to checking if an
203 edge is obstacle-free by sampling along the edge and checking if the samples are all within X_{free} .204 The modified *BidirectionalRRT** is presented in Algorithm 2. In lines 1, 2, we initialize the final
205 path as currently being none, and the corresponding cost to be infinite. Subsequently, we perform the
206 following procedure over N samples: Beginning with \mathcal{G}_a — the graph starting at the origin - in lines 4,
207 5 we draw a randomly-selected point from X_{free} . Checking if the point lies within X_{free} is done using
208 Algorithm 1, and select the nearest point in the graph (we use an r-tree to accomplish this efficiently).
209 In line 6, create a point x_{new} that is closer to x_{rand} than $x_{nearest}$. Then in lines 7-9, select the r points in
210 \mathcal{G}_a that are nearest to x_{new} and sort them in order of increasing distance from x_{new} , where the sorted
211 list L_s consists of tuples of the form (x', c', σ') , where $x' \in X_{near}$, σ' is an edge from x' to x_{new} , and c' is
212 the cost of that path, and select the closest one with an obstacle-free path to x_{new} as in [60]. If there is a
213 valid “best parent” — defined as the vertex with the lowest combined cost-to-come and cost-to-go -

Algorithm 1: CollisionCheck

Input : Point x ; Number of operators p ; robots \mathcal{A}
Output: True if obstacle-free, False otherwise

```

1  $n_{colls} \leftarrow 0$ 
2 for  $i \in [1, m]$  do
3    $q \leftarrow \lambda^i(x_i)$  if  $q \in \mathcal{C}_{att}^i$  then
4      $n_{colls} \leftarrow n_{colls} + 1$ 
5     if  $n_{colls} \geq p$  then
6       | return False
7     end
8   end
9 end
10 return True

```

214 we insert it into the graph and rewire as in [60] (lines 10-13). We then attempt to connect both trees. In
 215 lines 14-17, we select the nearest vertex in the opposite graph \mathcal{G}_b and attempt to draw a straight path
 216 from the newly-added vertex $x_{new} \in \mathcal{G}_a$ to \mathcal{G}_b , if possible. We then check if the resulting path is better
 217 than our current best-path σ_{best} and update σ_{best} if necessary.

218 At this point in the algorithm, we may have a valid path σ_{best} through X_{free} . We then perform
 219 *RandomContraction* as in [60] to attempt reducing the length of σ_{best} . The user may assign a probability
 220 p_{early} , corresponding to the likelihood of checking for an early-exit solution; this is to balance between
 221 the run-time of *B-RRT** and yielding a better path. We evaluate this in lines 20-23, returning a valid
 222 solution if one exists. Otherwise, we swap \mathcal{G}_a and \mathcal{G}_b and continue until all N samples have been
 223 drawn and return σ_{best} .

224 We then proceed by mapping h to the sequence of configurations \tilde{x}^i that correspond to robot \mathcal{A}^i .
 225 Movement parallel to an axis corresponds to that robot moving at full speed, perpendicular segments
 226 indicate the robot is paused, and diagonal segments to velocity-tuning depending on the slope.

227 To the best of our knowledge, our approach is one of the first to use geometric and motion
 228 planning techniques to schedule operators' attention. Since most previous methods are based on
 229 human factor techniques or combinatorial scheduling algorithms, head-to-head comparison is difficult.
 230 Furthermore, our study cases (multi-robot control and humanoid manipulation) are different from the
 231 ones presented in related work (e.g., foraging [27]). In the near term, one direction for comparison
 232 would be applying our techniques to previously used study cases and benchmark the approach.

233 We believe that our proposed method has a good scaling behavior. An additional robot and
 234 its constraints represent an additional variable in our coordination space. Since we are using
 235 sampling-based methods for finding a feasible solution (which have been used in large dimensions [61]),
 236 we believe that our method can scale to larger groups. Furthermore, in sampling-based motion
 237 planning, a significant part of the computational cost is collision checking, and since this is simple in
 238 our formulation (obstacles are hypercubes), there is good potential for scaling.

239 **5. Scheduling with Re-Planning**

240 The previous solution provides us with a coordination space and corresponding path that yields
 241 a velocity-tuning approach preventing operator collisions. We now look for a solution that yields a
 242 shorter mission runtime by also altering the robot trajectories. This solution is found by comparing the
 243 current path through the coordination space h and the desired shortest-path path h_{des} which would be
 244 a straight line. Given the example in Figure 2a, b, where we see the robots and environment, and the
 245 resulting coordination space, we indicate an "ideal" path as in Figure 2c. When searching for a path
 246 through the coordination space, we may find a point $x \in X$ such that $h_{des}(x) \cap X_{obs} \neq \emptyset$, representing
 247 an obstacle. In the example shown in Figure 2c, this is indicated by the blue region, meaning that the
 248 ideal path is not valid as it intersects the obstacle. In these situations, the solution is to either plan

Algorithm 2: *B-RRT**

Input :Coordination Space X , Operators p ; Critical Segments \mathcal{S} ; Samples N, Probability of early exit $p_{early} \in [0, 1]$

Output: Obstacle-free path σ_{best} through X

```

1  $\sigma_{best} \leftarrow \emptyset;$ 
2  $c_{best} \leftarrow \infty;$ 
3 for  $i \in [0, N]$  do
4    $x_{rand} \leftarrow SampleFree;$ 
5    $x_{nearest} \leftarrow Nearest(x_{rand}, \mathcal{G}_a);$ 
6    $x_{new} \leftarrow Extend(x_{nearest}, x_{rand});$ 
7    $X_{near} \leftarrow Near(x_{new}, \mathcal{G}_a, r);$ 
8    $L_s \leftarrow Sort(x_{new}, X_{near});$ 
9    $x_{min} \leftarrow BestParent(L_s);$ 
10  if  $x_{min} \neq \emptyset$  then
11    |  $\mathcal{G}_a \leftarrow Insert(x_{new}, x_{min}, \mathcal{G}_a);$ 
12    |  $\mathcal{G}_a \leftarrow Rewire(x_{new}, L_s, E);$ 
13  end
14   $x_{conn} \leftarrow Nearest(x_{new}, \mathcal{G}_b);$ 
15   $\sigma_{new} \leftarrow Connect(x_{new}, x_{conn}, \mathcal{G}_b);$ 
16  if  $\sigma_{new} \neq \emptyset$  and  $c(\sigma_{new}) < c(\sigma_{best})$  then
17    |  $\sigma_{best} \leftarrow \sigma_{new};$ 
18  end
19   $RandomContraction(\sigma_{best});$ 
20   $u \sim U([0, 1]);$ 
21  if  $\sigma_{best} \neq \emptyset$  and  $u \leq p_{early}$  then
22    | return  $\sigma_{best};$ 
23  end
24   $SwapTrees(\mathcal{G}_a, \mathcal{G}_b);$ 
25 end
26 return  $\sigma_{best};$ 

```

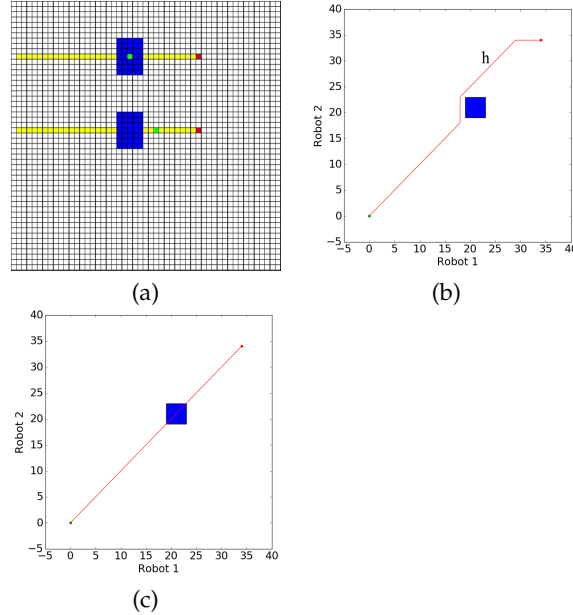


Figure 2. Example Environment and resulting Coordination Space

(a) A planar environment with dangerous regions requiring operator supervision to traverse shown in blue, and robot trajectories in yellow. (b) The 2-dimensional Coordination Space resulting from (a). Each axis corresponds to the positions of robots along with their trajectories. The red line indicates an attention-conflict-free path through the coordination space. (c) Coordination space from (b), with the desired (optimal) policy shown as the red line.

249 around the obstacle, corresponding to tuning the velocity of the robots involved - as in the solution
 250 for Problem 1 - or creating alternative plans for the robots. In the latter case, the number of operators
 251 requested during the original set of times corresponding to the obstacle can now be fulfilled, potentially
 252 reducing the overall mission runtime if the resulting plans are shorter than the wait times.

253 A critical side-effect to keep in mind is that by modifying robots' trajectories when avoiding
 254 collisions caused by conflicting operator attention requests, we are also potentially changing later parts
 255 of their trajectory. This change will lead to a different coordination space and the possibility of shifting,
 256 creating, or removing subsequent obstacles. As an illustrative example, Figure 3a shows two robots,
 257 which enter regions requiring supervision at the same time and produce the coordination space in
 258 Figure 3b. The vertical segment of the path h shown in red corresponds to the collision being resolved
 259 by pausing robot 1 until robot 2 has finished its operator request before continuing. This scenario
 260 could also be solved by re-planning robot 2 so that it avoids operator requests during the original
 261 times. However, robot 1 will then require more time to travel around the dangerous region, causing it
 262 to encounter its second critical section at a later time — precisely when robot 1 is entering its second
 263 request as well (Figure 3c) — creating another conflict that must be solved.

264 This setup yields our initial solution via velocity-tuning. Then create an ideal path h_{opt} , given
 265 by a straight line that assumes no robots require supervision (line 3). Next, we verify if the optimal
 266 solution is valid by checking for collisions between h_{des} and obstacles in the coordination space and
 267 return the first obstacle encountered — if any in line 4. *FirstObstacle* returns the robots involved in
 268 the “collision” $o_{A_{inv}}$, along with the corresponding configurations $o_{C_{att}}$ and times that each robot has in
 269 conflict $o_{t_{den}}$. If the ideal path is invalid (line 5), we can resolve this in two ways:

270 1. Alter the involved robots policies (as in the previous solution).
 271 2. Re-plan the involved robots trajectories to eliminate the obstacle.

272 We now describe how to re-plan the robot's trajectories. Given the robots involved in the collision,
 273 $o_{A_{inv}}$, we sort them in order of ascending length of execution time and select the shortest $|o_{A_{inv}}| - p$ -
 274 the minimum number of robots to re-plan to remove the attention collision (lines 6, 7). This procedure

Algorithm 3: Scheduler

Input : \mathcal{A} , robots to plan
Output: h , path through X used to derive policy

```

1  $x_{init} \leftarrow (0, \dots, 0); x_{goal} \leftarrow (\tilde{t}_f^1, \tilde{t}_f^m)$ 
2  $X_{curr} \leftarrow [\tilde{t}_f^1, \dots, \tilde{t}_f^m]; h_{curr} \leftarrow \text{B-RRT}^*(X_{curr}, x_{init}, x_{goal}, p, \mathcal{C}_{att})$ 
3  $X_{des} \leftarrow [0, \tilde{t}_f^1, \dots, \tilde{t}_f^m]; h_{des} \leftarrow \text{line}(x_{init}, x_{goal}); \mathcal{C}_{desatt} \leftarrow \emptyset$ 
4  $o \leftarrow \text{FirstObstacle}(h_{des}, \mathcal{C}_{att})$ 
5 while  $o \neq \emptyset$  do
6    $\mathcal{A}_{inv} \leftarrow \text{Sort}(o_{\mathcal{A}_{inv}})$ 
7    $\mathcal{A}_{min} \leftarrow \mathcal{A}_{inv}[0 : |o_{\mathcal{A}_{inv}}| - p]$ 
8    $\mathcal{A}_{alt} \leftarrow (\mathcal{A} \setminus \mathcal{A}_{min})$ 
9    $\text{plan}(\mathcal{A}^i, t_{den}^i) \forall \mathcal{A}^i \in \mathcal{A}_{min}$ 
10   $\mathcal{A}_{alt} \leftarrow \mathcal{A}_{alt} \cup \mathcal{A}_{min}$ 
11   $x_{altgoal} \leftarrow (\tilde{t}_f^1, \dots, \tilde{t}_f^m) \forall \mathcal{A}^i \in \mathcal{A}_{alt}$ 
12  if  $d(x_{init}, x_{altgoal}) \leq c(h_{curr})$  then
13     $X_{alt} \leftarrow [0, \tilde{t}_f^1] \times \dots \times [0, \tilde{t}_f^m]; h_{alt} \leftarrow \text{B-RRT}^*(X_{alt}, x_{init}, x_{goal}, p, \mathcal{C}_{att})$ 
14    if  $c(h_{alt}) \leq c(h_{curr})$  then
15       $x_{goal} \leftarrow x_{altgoal}; h_{curr} \leftarrow h_{alt}$ 
16       $X_{curr} \leftarrow X_{alt}; X_{des} \leftarrow X_{alt}$ 
17       $\mathcal{A} \leftarrow (\mathcal{A} \setminus \mathcal{A}_{min}) \cup \mathcal{A}_{alt}$ 
18    else
19       $\mathcal{C}_{desatt} \leftarrow \mathcal{C}_{desatt} \cup o_{\mathcal{C}_{att}}$ 
20    end
21  else
22     $\mathcal{C}_{desatt} \leftarrow \mathcal{C}_{desatt} \cup o_{\mathcal{C}_{att}}$ 
23  end
24   $h_{des} \leftarrow \text{B-RRT}^*(X_{des}, x_{init}, x_{goal}, p, \mathcal{C}_{att})$ 
25   $o \leftarrow \text{FirstObstacle}(h_{des}, \mathcal{C}_{att})$ 
26 end
27 return  $h_{des}$ 

```

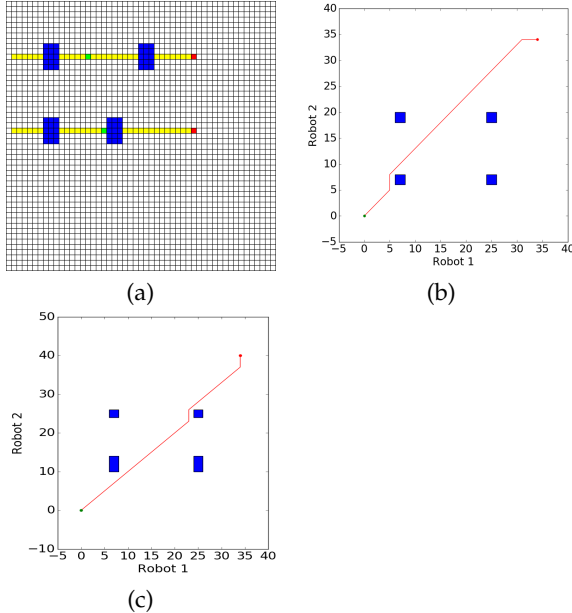


Figure 3. Example Environment, resulting Coordination Space, and Shifting Conflict Regions

(a) Robots in their environment, and their expected trajectories; (b) Original Coordination Space resulting from (a); (c) Final Coordination Space after re-planning around the first attention obstacle.

275 is performed on the robots with the shortest current plans so that extensions to their plans due to
 276 re-planning should have a minimal effect on the mission's overall length. Then generate alternative
 277 trajectories for the robots, provided operator-denied times $o_{t_{den}}$, and create an alternative goal location
 278 $x_{altgoal}$ to account for any shifts in the ending times of the robot plans (lines 8 - 11).

279 Suppose the distance between x_{init} and the alternative $x_{altgoal}$ is longer than the current solution.
 280 In that case, velocity-tuning will yield a better solution, and we incorporate the obstacle into the
 281 "desired" set of obstacles (lines 12, 22). Otherwise, we test if the alternative, a re-planned solution is
 282 better (lines 13, 14). If it is, then update the robots with their re-planned trajectories, and replace the
 283 current coordination space and goal to account for any changes in execution times (lines 15 - 17); else
 284 we incorporate the obstacle into the "desired" set of obstacles as before (line 19).

285 We repeat this process of generating desired solutions (line 24) and testing them until the desired
 286 path h_{des} no longer intersects any obstacles. At this point, we return the final h_{des} that will have no
 287 operator conflicts.

288 6. Experimental Results

289 In this section, we cover the design and of both simulated and physical experiments, and the
 290 results obtained.

291 6.1. Software Simulation for Scheduling with Re-Planning

292 Here we describe our simulation and provide an example *plan* algorithm that re-plans a robot's
 293 trajectory around unsafe areas in the environment — which would require operator supervision
 294 — given operator-denied times.

295 The simulated environment consisted of a discretized 2-dimensional grid-world where robots can
 296 only move either horizontally or vertically. The environment also contains hazardous regions (shown
 297 in blue) which require operator supervision to traverse, corresponding to configurations in \mathcal{C}_{att} .

298 **Example Re-plan Algorithm:** The *plan* algorithm used in this example attempts to find the
 299 shortest path between x_{init}^i and x_{final}^i within the robot's environment, which can be easily attained via
 300 the *A** algorithm [62,63]. However, this path may intersect with regions requiring supervision. First,

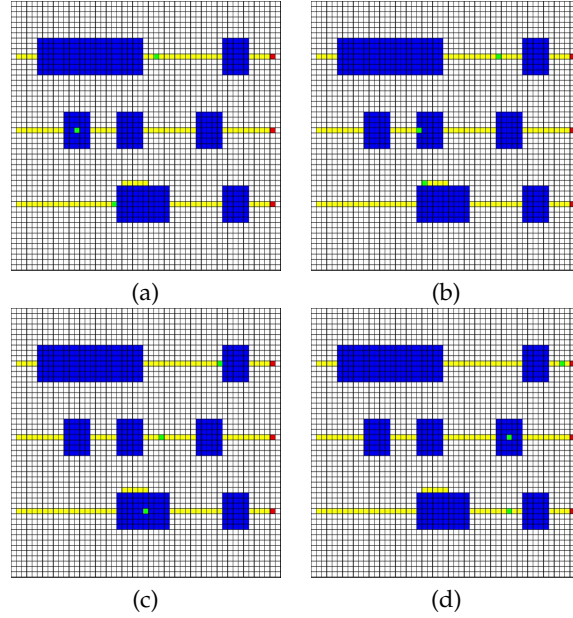


Figure 4. Example Simulation Environment

Example simulation. The robots are numbered 1, 2, 3 from top to bottom. (a) Robot 3 stops while Robot 2 passes through its dangerous region. (b) Robot 3 has re-planned its trajectory and is going around the dangerous area, allowing Robot 2 to be supervised. (c) Robot 1 stops to allow Robot 3 enter its dangerous area with supervision. (d) All robots continue to their final goal locations.

301 denote the starting time of the mission as $T_i = 0$. Given times when an operator will not be available
 302 for the robot, t_{den} , we modify A^* as follows: Augment A^* 's nodes with an additional *time* parameter.
 303 When visiting a node, update its neighbor's *time* attributes to *time* + *travel_time* where *time* is the
 304 current time, and *travel_time* is the time required to move from the current node to the neighbor. If
 305 the neighbor physically resides within C_{att} and the neighbors *time* is inside t_{den} , then we treat it as an
 306 obstacle. This modification of A^* provides paths that circumvent obstacles during operator-denied
 307 times, with an example shown in Figure 4.

308 In Figure 4, we show a simulated example given an environment with three robots. The blue
 309 areas in the environment are dangerous, and require operator supervision to prevent an accident. The
 310 example was designed to show several operator attention “collision” scenarios. As the robots move
 311 from left to right, the following operator requests might arise:

312

- \mathcal{A}^1 requiring an operator
- \mathcal{A}^1 and \mathcal{A}^2 require an operator at the same time
- $\mathcal{A}^1, \mathcal{A}^2, \mathcal{A}^3$ require an operator at the same time
- \mathcal{A}^3 requiring an operator while \mathcal{A}^1 and \mathcal{A}^2 leave their critical regions
- \mathcal{A}^2 requiring an operator
- \mathcal{A}^1 and \mathcal{A}^2 require an operator at the same time

318 The resulting coordination space is shown in Figure 5, where (a, b) is only velocity-tuning, and (c,
 319 d) is with re-planning the robot trajectories, which yields a slightly shorter mission ending time than
 320 strictly velocity-tuning.

321 For further validation, simulations were run using 2-dimensional environment populated with
 322 a set of randomly-sized, randomly-placed dangerous regions, and robots placed in randomized
 323 obstacle-free starting and goal locations along with a corresponding path between them as shown in
 324 Figure 6. Across each iteration of the simulations, environments and the starting and goal positions
 325 for the robots were randomly generated. In each generated environment, trials were run using 2, 4,
 326 or 8 robots, moving at 1 cell/second. These trials were then solved using the solutions for Problem 1

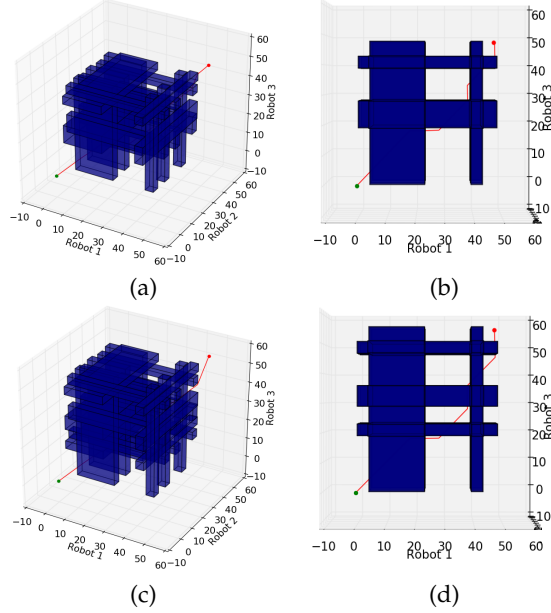


Figure 5. Example Simulation Coordination Space resulting from the example shown in Figure 4.

(a) Original Coordination Space resulting from the environment and robots in Figure 4; (b) Side view of (a); (c) Final Coordination Space after replanning; (d) Side view of (c)

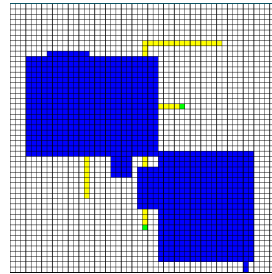


Figure 6. Example Random Environment

Example of a randomly-generated environment and trajectories intersecting critical regions.

Table 1. Average time savings via re-planning vs velocity-tuning

Robots	Operators	Average Savings
2	1	1.126
2	2	0
2	4	0
2	8	0
4	1	1.937
4	2	3.402
4	4	0
4	8	0
8	1	NA
8	2	0.218
8	4	5.284
8	8	0

³²⁷ (Scheduling) and Problem 2 (Scheduling with Re-Planning), with 1, 2, 4, or 8 operators. The results can
³²⁸ be found in Table 1.

³²⁹ There is an increase in average time saved when dealing with larger numbers of robots, as
³³⁰ re-scheduling can simultaneously resolve multiple robots at once. We purposefully ran the simulations
³³¹ with equal numbers of robots and operators to ensure that there would be no time saved - as there

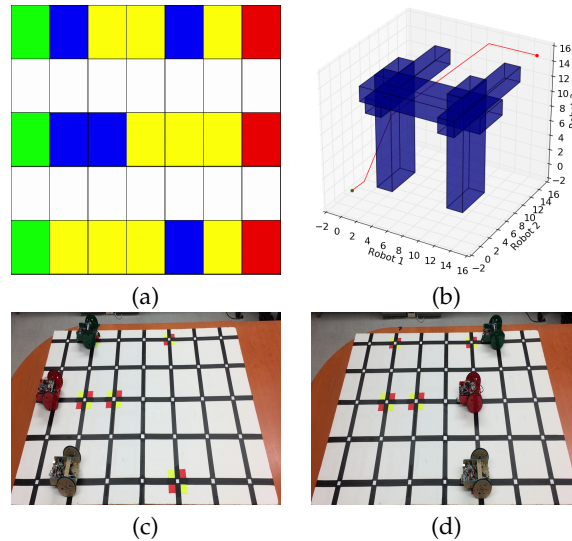


Figure 7. Hardware Experiment Example

(a) Simulated Environment; (b) Coordination Space resulting from (a); (c) Analogous hardware simulation at $t = 1$; (d) Hardware simulation at $t = 5$.

would be no obstacles generated in the first place - and this performed as expected. All tests with 2 and 4 robots completed successfully. In trials with 8 robots and single operator, a solution was not found with the RRT^* parameters that were used. Given 2 operators, 30% completed, and 60% for 4 operators. This result was due to the low sample count used when running Attention RRT^* , and the large *steer* length, which prevented it from exploring paths in narrow gaps between obstacles. The tuning of the sample count, steer length and rewire count lie outside the scope of this work, but is nonetheless an interesting problem we expect to incorporate in future work.

6.2. Hardware Experiment for Scheduling with Re-Planning

Here, we further illustrate the problem and solution via a hardware example. This example consisted of a single operator that had to be allocated across three line-following robots in a discrete grid environment.

The robots use a deterministic finite state machine to keep track of the position and orientation, and a transition function given by a second transition-state machine that ensures the robots inter-state path does not deviate from a grid line.

The hardware experiment in Figure 7 has an equivalent simulated environment shown in Figure 7a. The robots have initial trajectories shown in yellow, which pass through dangerous areas of the environment (blue) requiring operator supervision. The physical implementation represents the dangerous areas using red/yellow squares, in the same locations as in the virtual simulation. The resulting coordination space in Figure 7b, provides a set of policies enabling the robots to execute their trajectories while ensuring that the operator is not split among multiple robots at the same time. The robots then executed their corresponding policies, moving and pausing when appropriate, with at most one robot entering a dangerous region at a time. Additional experiments and videos can be found at:

<http://users.cis.fiu.edu/jabobadi/oa/>.

The hardware experiments that were run and shown in the above link show successful runs using the above procedures to design trajectories and policies for three different robots under the supervision of a single operator. The mission ended in the shortest time possible, and the operator did not receive multiple concurrent requests.

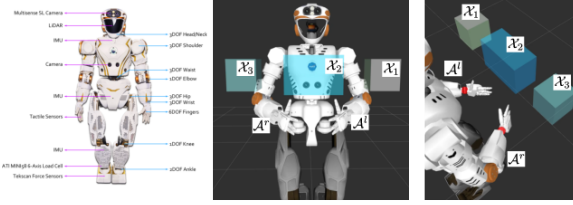


Figure 8. (Left) NASA's humanoid robot Valkyrie. (Middle, Right) Experimental setup showing coordination space obstacles and kinematic chains that are treated as independent robots.

361 7. Study Case: Humanoid Robots

362 In this section, an application of the proposed method to NASA's humanoid robot Valkyrie [64]
 363 as shown Fig. 8, is presented. Humanoid robots are high degree of freedom complex systems that
 364 have been proposed for diverse applications including nuclear-decommissioning tasks [65,66], disaster
 365 response assistance [67], and vehicles of space exploration [64]. For many of these tasks, it is desirable
 366 to have a *human-in-the-loop* controller to ensure critical and hazardous sub-tasks are completed. The
 367 supervised autonomy frameworks to make humanoid robots applicable in performing complex tasks
 368 require an effective design for a shared operator control interface which remains an open question.
 369 As seen during the DRC, completion of complex tasks in simulated environments with humanoids
 370 requires large teams of operators and shared control is indispensable [67]. Indeed even a simple
 371 manipulation task requires coherent operator collaboration or inter-operator communication problems
 372 can have detrimental effects [9]. Thus it is preferable to enforce a 1:1 ratio between humanoids and
 373 operator [8].

374 7.1. Methodology

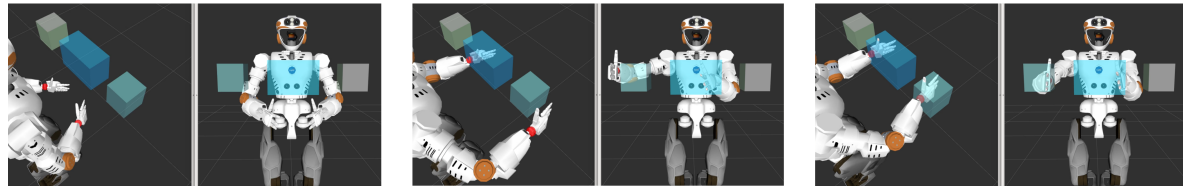
We propose partitioning the humanoid robot into two serial kinematic chains, the left and right arm, which are denoted as \mathcal{A}^l and \mathcal{A}^r respectively. The desired task is modeled as a typical pick and place operation where the robots must visit designated picking and placing zones defined by the bounding boxes $\mathcal{X}_{i=1\dots n}$. For example, \mathcal{A}^r picks an object from \mathcal{X}_1 and places it in \mathcal{X}_2 . Next, \mathcal{A}^l collects the object from \mathcal{X}_2 and places it in a final location \mathcal{X}_3 . The picking and placing actions are executed by the end effectors of the right and left arms whose positions are respectively given by \mathbf{p}^r and \mathbf{p}^l . When an end effector (robot's hand) is within a bounding box $\mathcal{X}_{i=1\dots n}$, it requires operator attention, i.e., the action is considered sensitive and require operator supervision. Thus $\mathcal{X}_{i=1\dots n}$ constitute configuration space constraints that must be transformed into critical regions in the coordination space. Thus, the constraints are represented in the configuration space as follows:

$$\lambda^l(t) \cap \lambda^r(t) = \emptyset \mid \forall t \in [0, t_f]; \lambda^l(t), \lambda^r(t) \in \mathcal{X}$$

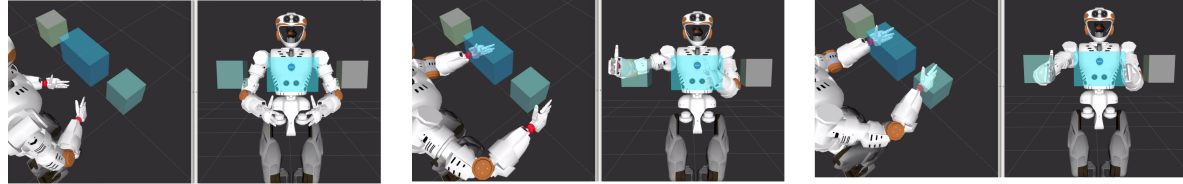
375 Additionally, the re-planning algorithm is modified as follows: Given a set of waypoints τ and
 376 operator-denied times t_{den} , *plan* will re-plan sections of λ that reside within \mathcal{X} during times t_{den} if
 377 possible. If re-planning is not possible, or if there are critical waypoints that should not be altered
 378 (such as waypoints denoting pick and place actions) the waypoints and relevant sections of λ will be
 379 untouched and returned to the scheduler as-is.

380 7.2. Results

381 The simulation experiments are executed using the dynamic simulator *Gazebo*. An initial set of
 382 waypoints are defined for \mathcal{A}^l and \mathcal{A}^r . These waypoints consist of a set of Cartesian positions and
 383 velocities for the kinematic chains such that λ^r and λ^l satisfy the pick and place task constraints. The
 384 initial waypoints are passed to the scheduling algorithm which generates a new set of waypoints
 385 that - when separated by a monotonic time step - satisfy both the configuration and coordination



(a) Initial trajectory with three attention zones

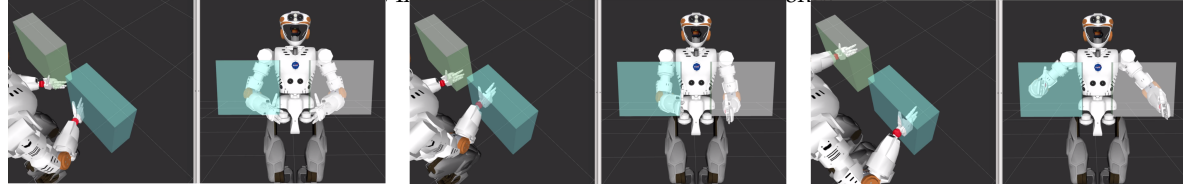


(b) Rescheduled and re-planned trajectory with three attention zones

Figure 9. Pick and place task with three attention obstacles. The planning reference frame is located at the wrist of the respective arms and is highlighted by a red square. Left: Both plans start in a valid position. Middle: Both plans approach the bounding in the same manner, but in the rescheduled case, the right arm execution is slowed down to ensure that before entering the bounding box the left hand has already left the attention zone (Right).



(a) Initial trajectory with two attention zones



(b) Rescheduled and re-planned trajectory with two attention zones

Figure 10. Pick and place task with two attention obstacles. The planning reference frame is located at the wrist of the respective arms and is highlighted by a red square. Left: Both plans start in a valid position. Middle: The initial trajectory immediately violates attention constraints while the rescheduled trajectory slows the left arm to prevent entry into the area. Right: The right arm is slightly withdrawn (re-planning) to ensure target frame is outside the bounding box before the left has to enter.

386 space constraints. A cubic interpolation of the waypoints is used to generate a continuous trajectory
 387 for execution on the robot. A comparison between the executions before and after the scheduling
 388 algorithm is shown in Figure 9 and Figure 10. The coordination space of these trajectories is shown in
 389 Figure 11.

390 The two original trajectories shown in Figures 11a and 11b have conflicts in critical areas as
 391 illustrated by the line passing through purple areas. The reduced purple areas in Figures 11c and 11d
 392 demonstrate the re-planning of waypoints, and the altered slope of the line through space indicates
 393 a change in time through the waypoints. Both trajectories use a combination of re-planning and
 394 rescheduling to generate a collision-free path through the coordination space.

395 8. Conclusions and Future Work

396 This work provides a geometric approach for converting robot trajectories and supervision
 397 requests into a set of policies for the robots that permit operators to oversee critical sections of robot
 398 plans without being over-allocated. The provided solution is also capable of determining when

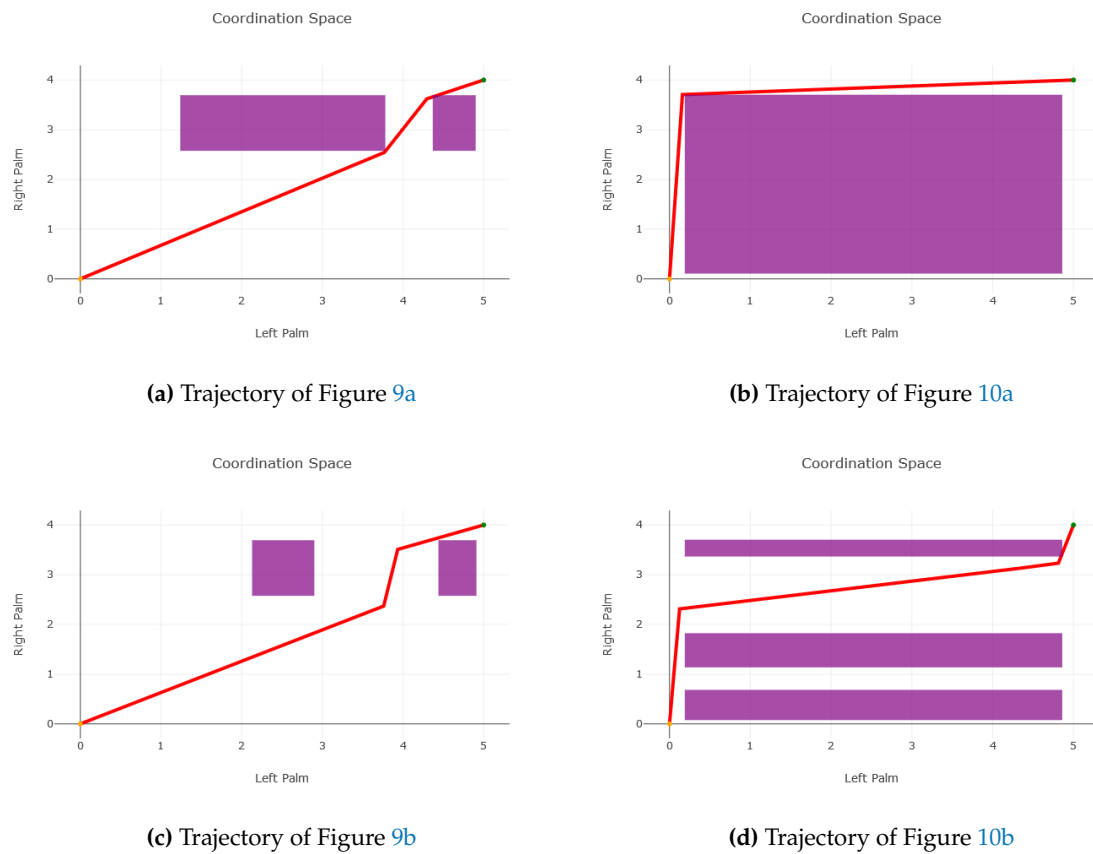


Figure 11. Purple areas represent times when both palms will be in a critical zone while the red line is the scheduled times to reach a point for each palm.

399 re-planning robots would yield a better solution than velocity-tuning. [There are exciting avenues for](#)
 400 [future work.](#)

401 In the short term, we would like to look at the effects that robot movement has on an operator's
 402 effectiveness in overseeing them [68], and incorporate this effect into our solution. As an example,
 403 operators require time to switch their attention from one robot to another. This context switching time
 404 might be represented by extending obstacles in the coordination space towards the origin. Similarly, a
 405 robot's path may have some element of uncertainty, especially when outside of a factory setting. In
 406 this case, we can "inflate" the obstacles within the coordination space, which would provide a more
 407 cautious solution.

408 We are also interested in improving our modeling of context switching times by using
 409 constructions from Human-Robot Interaction research. Potential sources of information that can
 410 be incorporated are mental states (MS) modeling and physiological factors [30]. We believe that the
 411 combination of realistic human cognition models and algorithmic, scalable methodologies such as the
 412 one we proposed in this paper can lead to fundamental insights.

413 Searching through the coordination space might be modified to use a receding horizon approach
 414 to allow for more rapidly changing robot plans if presented with a dynamic environment. We would
 415 like to include the stability constraints and interdependence between kinematic chains when working
 416 with robots with large degree of freedom.

417 We studied the complexity of problem 1 and argued that it is NP-Hard by using the technique or
 418 restriction, and we proceeded to propose feasible heuristics to solve it. A natural direction will be to
 419 carefully study approximation algorithms [69] for scheduling problems [70] that can be translated into
 420 our framework. This can help us calculate approximation ratios and performance guarantees for our
 421 approach.

422 In our paper, we have presented two study cases to show our approach's practical feasibility
423 and range of applications. The first scenario is on a set of mobile robots, and the second is on a robot
424 with several degrees of freedom. We want to continue exploring applications and extend this work to
425 human studies to investigate the framework's effectiveness for complex teleoperation tasks. A domain
426 of interest where our ideas can apply are one-to-many (OTM) scenarios where a human operator needs
427 to monitor and coordinate multiple multiple autonomous vehicles [39].

428 **Author Contributions:** "Conceptualization, Sebastián Zanlongo, Philip Long, Leonardo Bobadilla and Taskin
429 Padir; Methodology, Sebastián Zanlongo, Philip Long and Leonardo Bobadilla; Software, Peter Dirksmeier,
430 Sebastián Zanlongo, Philip Long and Leonardo Bobadilla; Validation, Sebastián Zanlongo and Peter Dirksmeier;
431 Writing—original draft preparation, Sebastián Zanlongo, Philip Long, Leonardo Bobadilla; Writing—review and
432 editing, Philip Long, Leonardo Bobadilla and Taskin Padir; Supervision, Philip Long, Leonardo Bobadilla
433 and Taskin Padir; Project administration Leonardo Bobadilla and Taskin Padir; Funding acquisition, Leonardo
434 Bobadilla and Taskin Padir".

435 **Funding:** This research is supported by the Department of Energy under Award Number DE-EM0004482, by the
436 National Aeronautics and Space Administration under Grant No. NNX16AC48A issued through the Science and
437 Technology Mission Directorate and by the National Science Foundation under Award No. 1451427. This research
438 is also supported in part by the National Science Foundation through awards IIS-2034123 and IIS-2024733 and by
439 the U.S. Department of Homeland Security under Grant Award Numbers 2017-ST-062000002.

440 **Conflicts of Interest:** The authors declare no conflict of interest.

441 Abbreviations

442 The following abbreviations are used in this manuscript:

444 RRT Rapidly Exploring Random Tree

445 References

- 446 1. Alam, T.; Bobadilla, L. Multi-Robot Coverage and Persistent Monitoring in Sensing-Constrained
447 Environments. *Robotics* **2020**, *9*, 47.
- 448 2. Bandala, M.; West, C.; Monk, S.; Montazeri, A.; Taylor, C.J. Vision-based assisted tele-operation of a
449 dual-arm hydraulically actuated robot for pipe cutting and grasping in nuclear environments. *Robotics*
450 **2019**, *8*, 42.
- 451 3. Murphy, R.R.; Gandudi, V.B.M.; Adams, J. Applications of robots for Covid-19 response. *arXiv preprint
452 arXiv:2008.06976* **2020**.
- 453 4. Shah, J.; Wiken, J.; Williams, B.; Breazeal, C. Improved human-robot team performance using chaski,
454 a human-inspired plan execution system. 6th international conference on Human-robot interaction. ACM,
455 2011, pp. 29–36.
- 456 5. Wilcox, R.; Nikolaidis, S.; Shah, J. Optimization of temporal dynamics for adaptive human-robot interaction
457 in assembly manufacturing. *Robotics Science and Systems VIII* **2012**, pp. 441–448.
- 458 6. Helms, E.; Schraft, R.D.; Hagele, M. rob@ work: Robot assistant in industrial environments. IEEE
459 International Workshop on Robot and Human Interactive Communication. IEEE, 2002, pp. 399–404.
- 460 7. Murphy, R.R. Human-robot interaction in rescue robotics. *IEEE Transactions on Systems, Man, and
461 Cybernetics, Part C (Applications and Reviews)* **2004**, *34*, 138–153.
- 462 8. Yanco, H.A.; Norton, A.; Ober, W.; Shane, D.; Skinner, A.; Vice, J. Analysis of human-robot interaction at
463 the darpa robotics challenge trials. *Journal of Field Robotics* **2015**, *32*, 420–444.
- 464 9. Atkeson, C.G.; Benzun, P.B.; Banerjee, N.; Berenson, D.; Bove, C.P.; Cui, X.; DeDonato, M.; Du, R.; Feng,
465 S.; Franklin, P.; others. What happened at the DARPA robotics challenge finals. In *The DARPA Robotics
466 Challenge Finals: Humanoid Robots to the Rescue*; Springer, 2018; pp. 667–684.
- 467 10. Zanlongo, S.A.; Rahman, M.; Abodo, F.; Bobadilla, L. Multi-robot Planning for Non-overlapping Operator
468 Attention Allocation. IEEE International Conference on Robotic Computing. IEEE, 2017, pp. 109–112.
- 469 11. Zanlongo, S.; Abodo, F.; Long, P.; Padir, T.; Bobadilla, L. Multi-Robot Scheduling and Path-Planning for
470 Non-Overlapping Operator Attention. 2018 Second IEEE International Conference on Robotic Computing
(IRC). IEEE, 2018, pp. 87–94.

472 12. Sandoval Arévalo, J.S.; Laribi, M.A.; Zeghloul, S.; Arsicault, M. On the design of a safe human-friendly
473 teleoperated system for doppler sonography. *Robotics* **2019**, *8*, 29.

474 13. Lasota, P.A.; Fong, T.; Shah, J.A.; others. *A survey of methods for safe human-robot interaction*; Now Publishers,
475 2017.

476 14. Sun, D.; Liao, Q.; Loutfi, A. Single master bimanual teleoperation system with efficient regulation. *IEEE
477 Transactions on Robotics* **2020**, *36*, 1022–1037.

478 15. Li, Y.; Liu, K.; He, W.; Yin, Y.; Johansson, R.; Zhang, K. Bilateral teleoperation of multiple robots under
479 scheduling communication. *IEEE Transactions on Control Systems Technology* **2019**, *28*, 1770–1784.

480 16. Rosenberg, L.B. The Use of Virtual Fixtures as Perceptual Overlays to Enhance Operator Performance in
481 Remote Environments. Technical report, Stanford Univ Ca Center for Design Research, 1992.

482 17. Bowyer, S.A.; Davies, B.L.; y Baena, F.R. Active constraints/virtual fixtures: A survey. *IEEE Transactions on
483 Robotics* **2014**, *30*, 138–157.

484 18. Yamamoto, T.; Abolhassani, N.; Jung, S.; Okamura, A.M.; Judkins, T.N. Augmented reality and haptic
485 interfaces for robot-assisted surgery. *The International Journal of Medical Robotics and Computer Assisted
486 Surgery* **2012**, *8*, 45–56.

487 19. Bettini, A.; Marayong, P.; Lang, S.; Okamura, A.M.; Hager, G.D. Vision-assisted control for manipulation
488 using virtual fixtures. *IEEE Transactions on Robotics* **2004**, *20*, 953–966.

489 20. Quintero, C.P.; Dehghan, M.; Ramirez, O.; Ang, M.H.; Jagersand, M. Flexible virtual fixture interface for
490 path specification in tele-manipulation. 2017 IEEE International Conference on Robotics and Automation
491 (ICRA). IEEE, 2017, pp. 5363–5368.

492 21. Pruks, V.; Farkhatdinov, I.; Ryu, J.H. Preliminary study on real-time interactive virtual fixture generation
493 method for shared teleoperation in unstructured environments. International Conference on Human
494 Haptic Sensing and Touch Enabled Computer Applications. Springer, 2018, pp. 648–659.

495 22. Long, P.; Keleştemur, T.; Önol, A.Ö.; Padir, T. optimization-Based Human-in-the-Loop Manipulation Using
496 Joint Space Polytopes. 2019 International Conference on Robotics and Automation (ICRA). IEEE, 2019, pp.
497 204–210.

498 23. Farkhatdinov, I.; Ryu, J.H. Teleoperation of multi-robot and multi-property systems. 2008 6th IEEE
499 International Conference on Industrial Informatics. IEEE, 2008, pp. 1453–1458.

500 24. Roldán, J.J.; Díaz-Maroto, V.; Real, J.; Palafox, P.R.; Valente, J.; Garzón, M.; Barrientos, A. Press start to play:
501 Classifying multi-robot operators and predicting their strategies through a videogame. *Robotics* **2019**, *8*, 53.

502 25. Luo, J.; Lin, Z.; Li, Y.; Yang, C. A teleoperation framework for mobile robots based on shared control. *IEEE
503 Robotics and Automation Letters* **2019**, *5*, 377–384.

504 26. Hughes, T. Human-Automation Coordination in Multi-UAV Control. AIAA Guidance, Navigation and
505 Control Conference and Exhibit, 2008, p. 6315.

506 27. Chien, S.Y.; Lewis, M.; Mehrotra, S.; Brooks, N.; Sycara, K. Scheduling operator attention for multi-robot
507 control. 2012 IEEE/RSJ International Conference on Intelligent Robots and Systems. IEEE, 2012, pp.
508 473–479.

509 28. Dardona, T.; Eslamian, S.; Reisner, L.A.; Pandya, A. Remote presence: development and usability
510 evaluation of a head-mounted display for camera control on the da Vinci Surgical System. *Robotics* **2019**,
511 *8*, 31.

512 29. Wong, C.Y.; Seet, G. Workload, awareness and automation in multiple-robot supervision. *International
513 Journal of Advanced Robotic Systems* **2017**, *14*, 1729881417710463.

514 30. Roy, R.N.; Drougard, N.; Gateau, T.; Dehais, F.; Chanel, C.P. How Can Physiological Computing Benefit
515 Human-Robot Interaction? *Robotics* **2020**, *9*, 100.

516 31. Dybvik, H.; Løland, M.; Gerstenberg, A.; Slåttsveen, K.B.; Steinert, M. A low-cost predictive display
517 for teleoperation: Investigating effects on human performance and workload. *International Journal of
518 Human-Computer Studies* **2021**, *145*, 102536.

519 32. Lu, S.; Zhang, M.Y.; Ersal, T.; Yang, X.J. Workload management in teleoperation of unmanned ground
520 vehicles: Effects of a delay compensation aid on human operators' workload and teleoperation performance.
521 *International Journal of Human-Computer Interaction* **2019**, *35*, 1820–1830.

522 33. Riley, J.M.; Endsley, M.R. Situation awareness in HRI with collaborating remotely piloted vehicles.
523 proceedings of the Human Factors and Ergonomics Society Annual Meeting. SAGE Publications Sage CA:
524 Los Angeles, CA, 2005, Vol. 49, pp. 407–411.

525 34. Adams, J.A. Multiple robot/single human interaction: Effects on perceived workload. *Behaviour &*
526 *Information Technology* **2009**, *28*, 183–198.

527 35. Al-Hussaini, S.; Gregory, J.M.; Guan, Y.; Gupta, S.K. Generating Alerts to Assist With Task Assignments
528 in Human-Supervised Multi-Robot Teams Operating in Challenging Environments. IEEE International
529 Conference on Intelligent Robots and Systems, 2020.

530 36. Al-Hussaini, S.; Gregory, J.M.; Shriyam, S.; Gupta, S.K. An Alert-Generation Framework for Improving
531 Resiliency in Human-Supervised, Multi-Agent Teams. *arXiv preprint arXiv:1909.06480* **2019**.

532 37. Velagapudi, P.; Scerri, P.; Sycara, K.; Wang, H.; Lewis, M.; Wang, J. Scaling effects in multi-robot control.
533 2008 IEEE/RSJ International Conference on Intelligent Robots and Systems. IEEE, 2008, pp. 2121–2126.

534 38. Prewett, M.S.; Johnson, R.C.; Saboe, K.N.; Elliott, L.R.; Covert, M.D. Managing workload in human–robot
535 interaction: A review of empirical studies. *Computers in Human Behavior* **2010**, *26*, 840–856.

536 39. Lim, Y.; Pongsarkornsathien, N.; Gardi, A.; Sabatini, R.; Kistan, T.; Ezer, N.; Bursch, D.J. Adaptive
537 Human-Robot Interactions for Multiple Unmanned Aerial Vehicles. *Robotics* **2021**, *10*, 12.

538 40. Parker, L. Multiple mobile robot systems. In *Springer Handbook of Robotics*; Springer, 2008; pp. 921–941.

539 41. Ponda, S.; Johnson, L.; Geramifard, A.; How, J. Cooperative mission planning for Multi-UAV teams. In
540 *Handbook of Unmanned Aerial Vehicles*; Springer, 2015; pp. 1447–1490.

541 42. Hauser, K. Minimum Constraint Displacement Motion Planning. *Robotics: Science and Systems*, 2013.

542 43. LaValle, S.; Hutchinson, S. Optimal Motion Planning for Multiple Robots Having Independent Goals. IEEE
543 International Conference on Robotics and Automation, 1996, pp. 2847–2852.

544 44. LaValle, S.; Hutchinson, S. Optimal Motion Planning for Multiple Robots Having Independent Goals. *IEEE
545 Transactions on Robotics and Automation* **1998**, *14*, 912–925.

546 45. Wang, J.; Zhang, Y.; Geng, L.; Fuh, J.; Teo, S. Mission planning for heterogeneous tasks with heterogeneous
547 UAVs. International Conference on Control Automation Robotics & Vision (ICARCV). IEEE, 2014, pp.
548 1484–1489.

549 46. Crandall, J.; Cummings, M.; Della Penna, M.; de Jong, P.M. Computing the effects of operator attention
550 allocation in human control of multiple robots. *IEEE Transactions on Systems, Man, and Cybernetics-Part A:
551 Systems and Humans* **2011**, *41*, 385–397.

552 47. Cummings, M.; Mitchell, P. Operator scheduling strategies in supervisory control of multiple UAVs.
553 *Aerospace Science and Technology* **2007**, *11*, 339–348.

554 48. Murphy, R.; Shields, J. The role of autonomy in DoD systems. Technical report, Technical report,
555 Department of Defense, Defense Science Board Task Force Report, 2012.

556 49. Ramchurn, S.; Fischer, J.; Ikuno, Y.; Wu, F.; Flann, J.; Waldock, A. A study of human-agent collaboration for
557 multi-UAV task allocation in dynamic environments **2015**.

558 50. Trautman, P. Probabilistic tools for human-robot cooperation. Human Agent Robot Teamwork Workshop
559 HRI, 2012.

560 51. Trautman, P.; Ma, J.; Murray, R.M.; Krause, A. Robot navigation in dense human crowds: Statistical models
561 and experimental studies of human–robot cooperation. *The International Journal of Robotics Research* **2015**,
562 *34*, 335–356.

563 52. Rahman, M.M.; Bobadilla, L.; Mostafavi, A.; Carmenate, T.; Zanlongo, S.A. An Automated Methodology for
564 Worker Path Generation and Safety Assessment in Construction Projects. *IEEE Transactions on Automation
565 Science and Engineering* **2018**, *15*, 479–491. doi:10.1109/TASE.2016.2628898.

566 53. Rahman, M.M.; Carmenate, T.; Bobadilla, L.; Zanlongo, S.; Mostafavi, A. A coupled discrete-event and
567 motion planning methodology for automated safety assessment in construction projects. *Robotics and
568 Automation (ICRA)*, 2015 IEEE International Conference on. IEEE, 2015, pp. 3849–3855.

569 54. Rahman, M.M.; Carmenate, T.; Bobadilla, L.; Mostafavi, A. Ex-ante assessment of struck-by safety hazards
570 in construction projects: A motion-planning approach. *Automation Science and Engineering (CASE)*, 2014
571 IEEE International Conference on. IEEE, 2014, pp. 277–282.

572 55. Gary, M.R.; Johnson, D.S. Computers and Intractability: A Guide to the Theory of NP-completeness, 1979.

573 56. LaValle, S. *Planning Algorithms*; Cambridge University Press: Cambridge, U.K., 2006. Also available at
574 <http://planning.cs.uiuc.edu/>.

575 57. Karaman, S.; Frazzoli, E. Sampling-based algorithms for optimal motion planning. *The international journal
576 of robotics research* **2011**, *30*, 846–894.

577 58. Karaman, S.; Frazzoli, E. Incremental sampling-based algorithms for optimal motion planning. *Robotics
578 Science and Systems VI* **2010**, *104*.

579 59. Jordan, M.; Perez, A. Optimal bidirectional rapidly-exploring random trees **2013**.

580 60. Qureshi, A.H.; Ayaz, Y. Intelligent bidirectional rapidly-exploring random trees for optimal motion
581 planning in complex cluttered environments. *Robotics and Autonomous Systems* **2015**, *68*, 1–11.

582 61. Shkolnik, A.; Tedrake, R. Path planning in 1000+ dimensions using a task-space Voronoi bias. 2009 IEEE
583 International Conference on Robotics and Automation. IEEE, 2009, pp. 2061–2067.

584 62. Beardwood, J.; Halton, J.; Hammersley, J. The shortest path through many points. Mathematical
585 Proceedings of the Cambridge Philosophical Society. Cambridge Univ Press, 1959, Vol. 55, pp. 299–327.

586 63. Matthews, J. Basic A* pathfinding made simple. *AI Game Programming Wisdom* **2002**, pp. 105–113.

587 64. Radford, N.A.; Strawser, P.; Hambuchen, K.; Mehling, J.S.; Verdeyen, W.K.; Donnan, A.S.; Holley, J.;
588 Sanchez, J.; Nguyen, V.; Bridgwater, L.; others. Valkyrie: Nasa’s first bipedal humanoid robot. *Journal of
589 Field Robotics* **2015**, *32*, 397–419.

590 65. Long, P.; Padir, T. Constrained Manipulability for Humanoid Robots Using Velocity Polytopes. *Int. J.
591 Humanoid Robotics* **2020**, *17*, 1950037–1.

592 66. Long, P.; Padir, T. Evaluating robot manipulability in constrained environments by velocity polytope
593 reduction. 2018 IEEE-RAS 18th International Conference on Humanoid Robots (Humanoids). IEEE, 2018,
594 pp. 1–9.

595 67. DeDonato, M.; Dimitrov, V.; Du, R.; Giovacchini, R.; Knoedler, K.; Long, X.; Polido, F.; Gennert, M.A.; Padir,
596 T.; Feng, S.; others. Human-in-the-loop Control of a Humanoid Robot for Disaster Response: A Report
597 from the DARPA Robotics Challenge Trials. *Journal of Field Robotics* **2015**, *32*, 275–292.

598 68. Koppengborg, M.; Nickel, P.; Naber, B.; Lungfiel, A.; Huelke, M. Effects of movement speed and
599 predictability in human–robot collaboration. *Human Factors and Ergonomics in Manufacturing & Service
600 Industries* **2017**, *27*, 197–209.

601 69. Vazirani, V.V. *Approximation algorithms*; Springer Science & Business Media, 2013.

602 70. Pinedo, M. *Scheduling*; Vol. 29, Springer, 2012.

603 © 2021 by the authors. Submitted to *Robotics* for possible open access publication under the terms and conditions
604 of the Creative Commons Attribution (CC BY) license (<http://creativecommons.org/licenses/by/4.0/>).